THE ASTROPHYSICAL JOURNAL, 201:256–262, 1975 October 15

OBSERVATIONS WITH A VLB ARRAY. II. THE SOURCES 4C 39.25, NRAO 150, VRO 42.22.01, 3C 345, AND 3C 454.3

D. B. SHAFFER
Yale University Observatory
M. H. COHEN, J. D. ROMNEY,* AND R. T. SCHILIZZI
Owens Valley Radio Observatory,† California Institute of Technology
K. I. KELLERMANN
National Radio Astronomy Observatory‡
G. W. SWENSON, JR.
University of Illinois
J. L. YEN
University of Toronto
AND
R. RINEHART
Harvard Radio Astronomy Station,§ Fort Davis, Texas
Received 1975 January 28; revised 1975 April 16

ABSTRACT

Three-antenna long-baseline interferometry at 10.7 GHz is reported for NRAO 150, 4C 39.25, 3C 345, VRO 42.22.01, and 3C 454.3 for several epochs between 1972 April and 1974 February. Simple models for the source brightness distributions fit the observations and indicate that most of the radio emission comes from one or two components. Component separations range up to ~50 lt-yr, and component sizes are on the order of 10 lt-yr. Small variations in source structure have been observed.

Subject headings: BL Lacertae objects — quasi-stellar sources or objects — radio sources, variable

I. INTRODUCTION

The preceding paper (Cohen *et al.* 1975, hereafter Paper I), describes the operation of a very-long-baseline (VLB) interferometer array at a frequency of ~10.7 GHz. This paper and the one that follows (Schilizzi *et al.* 1975, Paper III) present the results and our interpretations of the first six observing sessions. This paper discusses 4C 39.25, NRAO 150, VRO 42.22.01, 3C 345, and 3C 454.3, which can be modeled, as well as the data allow, by one or two components which supply most or all of the total 10.7 GHz flux density. For those sources with repeated observations, the structure seems to change slowly or not at all.

Model-fitting is discussed in Paper I. For the sources in this paper, we have restricted ourselves to models with only one or two Gaussian components. Two-component models typically determine 5 or 6 parameters: (1) flux density of the model (forced to be the total flux density for 4C 39.25, NRAO 150, and VRO 42.22.01), (2) ratio of component intensities, (3) and (4) sizes of components (constrained to be circular for the double models; "size" and "diameter" in § II refer to the full width at half-maximum [FWHM] of a Gaussian distribution), (5) and (6) separation and position angle between the components (the components of 3C 454.3 were constrained to be concentric). The first four of these parameters are usually highly correlated: considerable resolution of strong, large components is hard to distinguish from slight resolution of smaller, weaker components. There are several, if not many, models for all the sources; but the given models do represent the more significant features of the source brightness distributions.

II. THE SOURCES

Table 1 gives the optical identifications and redshifts for the sources discussed in this paper. Also included in Table 1 are the total flux densities (S_t) at the epochs of the several observing sessions, as measured at NRAO. We will refer to the various experiments by the session number in Table 1. Paper I gives further details about the experiments.

a) 4C 39.25

This source has the best-determined structure of any of the objects studied in this paper or in Paper III. The data for 4C 39.25 from sessions 1, 2, and 3 are presented in Figure 1. Session 6 had less than two hours of

* NSF Pre-doctoral Fellow.

† Supported by ONR contract N00014-67-A-0094-0019; also by NSF grants GP-30400-X1 and GP-19400.

‡ Operated by Associated Universities, Inc., under contract with the National Science Foundation.

§ Supported by NSF grant GP-8115.

TABLE 1

TOTAL FLUX DENSITIES

SOURCE	IDENTIFICATION	z	SESSIONS, DATES, AND STATIONS* 1 1972.33 FOG	2 1972.82 FOG	3 1973.21 FOGA	4 1973.46 GO	5 1973.55 FOB	6 1974.15 GO
NRAO 150	(0355+50) ...	...	8.75	9.15†	...	...	...	...
4C 39.25	(0923+39) QSO	0.698	10.9	11.4	12.5	...	...	10.2
3C 345	(1641+39) QSO	0.595	...	...	...	...	...	10.2
VRO 42.22.01	(2200+42) Galaxy	0.07‡	7.95	6.31	6.6:	...	...	...
3C 454.3	(2251+15) QSO	0.859	...	12.1	...	...	9.02	10.1:

NOTE.—Flux densities in janskys.

* F = Fort Davis (HRAS), O = OVRO, G = Green Bank (NRAO), A = ARO, B = Bonn (MPI). See Paper I for additional information about the individual experiments.

† Measured by B. H. Andrew.

‡ The redshift by Oke and Gunn (1974) has been disputed by Baldwin *et al.* 1975.

data for this source, and is not considered in the following discussion. The (u, v) coverage for session 1 is given in Figure 2. Two lines of maxima and a line of minima are drawn in Figure 2. The first (primary) maximum (labeled A), first minimum (a), and second maximum (B) are identified in Figures 1 and 2. The equally spaced extrema suggest a double structure for the source, and the amplitudes at A, a, and B provide other useful information. The amplitude ratio A/a gives an estimate of the relative strengths of the two components. Since $B < A$, the individual components are partially resolved, and their (average) size may be estimated. Parameters determined in this fashion are used as input to the modeling procedures described in Paper I.

Table 2 gives the best-fitting unequal double models for 4C 39.25 for sessions 1, 2, and 3. (For session 3, data from only the NRAO–OVRO and NRAO–HRAS baselines were used for model-fitting.) The two components provide the total 10.7 GHz flux density of the source. Circular components $\sim 0\overset{m}{.}0005$ in diameter give good fits. Elliptical components give slightly better fits, but we do not consider such results significant for these data. The solid lines in Figure 1 are the visibility curves calculated from the model for each session.

The range of separation and position angle values in Table 2 is consistent with the expected errors in determining these parameters from our data. There are no trends in these values, and the spacing and orientation

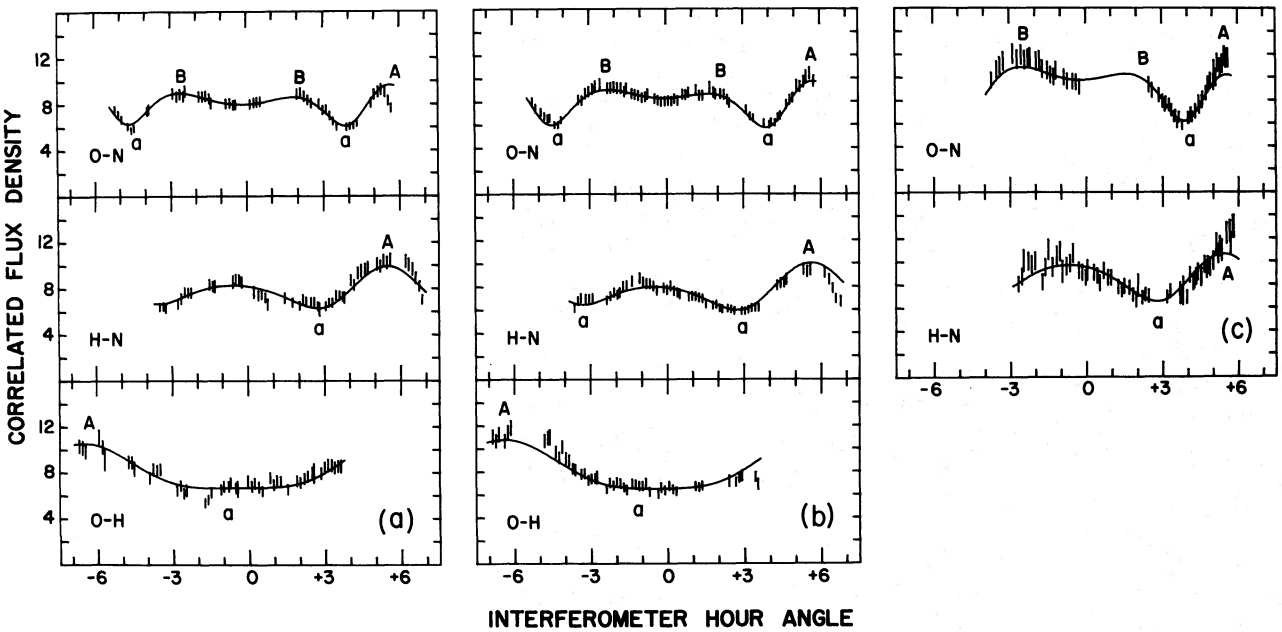

FIG. 1.—Fringe amplitude data for 4C 39.25. (a) = session 1, (b) = session 2, (c) = session 3. Ordinate is correlated flux density (Jy), abscissa is interferometer hour angle [hour angle from interferometer meridian (hours)]. Baselines are identified by antenna pairs: O = OVRO, H = HRAS, N = HRAO. A, a, and B locate the (u, v)-track crossings of the lines of maxima and minima identified in Fig. 2. The solid lines through the data are the calculated visibilities for the models given in Table 2.

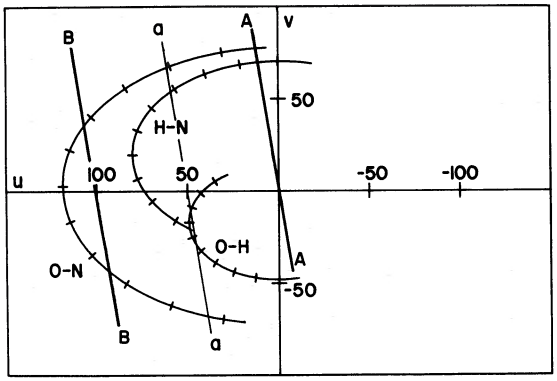

FIG. 2.—(u, v) tracks for 4C 39.25. Units are millions of wavelengths, with north up and east to the left. Tick marks on the curves are one hour apart. The loci of maxima (A and B) and minima (a) of the visibility function described by the models in Table 2 are indicated.

of the components of 4C 39.25 have not changed significantly during the period of these observations. The intensities of the individual components appear to be changing slowly, with the weaker component getting relatively stronger with time. Our more recent (unpublished) data show this trend to be continuing.

For $H = 55$ km s^{-1} Mpc^{-1} and $q_0 = 1$, the component separation is $\sim$40 lt-yr and the individual components are $\sim$10 lt-yr in size. These values of H and q_0 are assumed throughout this paper.

The data of Wittels *et al.* (1975) at 7.85 GHz are consistent with our model, both as to separation and orientation of the components. Additional observations at 7.85 GHz to measure the intensity ratio of the components would be useful for determining the spectra of the individual components.

TABLE 2

DOUBLE MODELS OF 4C 39.25

Session	Separation	Position Angle (degrees)	Intensity Ratio
1.....	0.″00203	99	4.2:1
2.....	0.00194	97	3.9:1
3.....	0.00207	101	3.9:1

NOTE.—The component sizes are $\sim$0.″0005.

b) NRAO 150

Our data for sessions 1 and 2 are given in Figure 3. The (u, v) coverage is not complete for either experiment, but the combined coverage is quite good (Fig. 4). For this high-declination source ($\delta \approx 50°$), the coverage is restricted by the hour-angle limits of the NRAO and HRAS telescopes. It is clear from the figures that we have not reached a definite minimum in the visibility function. This situation leads to an ambiguous interpretation of our data. Unless the normalized amplitude of the visibility function is observed to values $\lesssim 0.3$, it is impossible to distinguish among elliptical Gaussian, elliptical disk, and equal double brightness distributions.

The data for session 1 are fitted very well with an equal point double (0.″00060 separation in position angle [PA] 60°) or an elliptical Gaussian (0.″00076 × 0.″00015, major axis in PA 60°). Both models account for all the 10.7 GHz flux density. However, neither of these models fits the session 2 data particularly well.

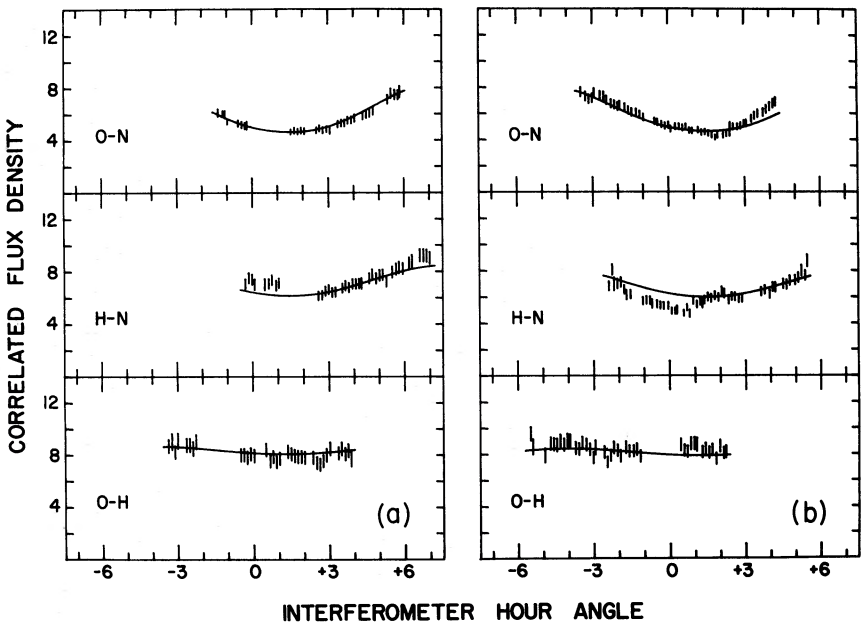

FIG. 3.—Fringe amplitude data for NRAO 150. (a) = session 1, (b) = session 2. Scales and baselines as in Fig. 1. The solid lines are the calculated visibilities for the models discussed in the text.

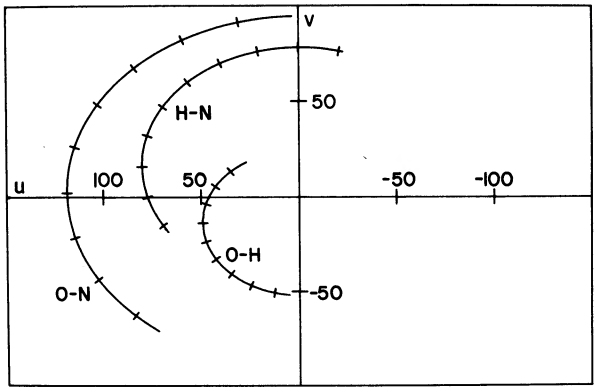

FIG. 4.—(u, v) tracks for NRAO 150. Scales as in Fig. 2.

Specifically, the models are about 10 percent too high on the HRAS–NRAO baseline. If a scaling error of this size existed (comparable to our claimed accuracy; Paper I), then either of these very simple models would fit the session 2 data with essentially no changes in the parameters.

It is possible to find more complicated models that give reasonable fits to both sets of data. An unequal double, with a $\sim$5.7 Jy point component (FWHM $\lesssim$ 0.″0003) and a $\sim$3.0 Jy $\sim$ 0.″0005 component, separated by 0.″00065 in PA 63°, is represented by the solid lines in Figure 3. This model accounts for all the session 1 flux density and 0.94 of the session 2 emission. There are some systematic differences between the models and the data, but it is unclear whether these differences are due to complexity of the source or calibration errors.

As with 4C 39.25, the structure of NRAO 150 shows no significant variation. Additionally, the structure is similar at 10.7 GHz and 7.85 GHz. Shaffer *et al.* (1972) and Wittels *et al.* (1975) give position angles for the greatest elongation of the source that are comparable to those found above. The models at 7.85 GHz are not well defined since the (u, v) coverage was very incomplete. Minor variations of the models suggested for the 10.7 GHz data will fit the 7.85 GHz data.

c) *VRO 42.22.01 (BL Lacertae)*

Extensive VLB observations at 7.85 GHz indicate that the radio structure of VRO 42.22.01 displays rapid changes (Clark *et al.* 1973; Wittels *et al.* 1975). The data of Clark *et al.* showed that the source was elongated in PA $\sim$175° and essentially unresolved in PA $\sim$84°. Clark *et al.* suggested a line component or multiple point components as possible models for the structure of the radio source. At 10.7 GHz the ambiguity remains, but we have been able to find a model that fits our data from two epochs.

The data from sessions 1 and 2 are displayed in Figure 5. The (u, v) tracks for VRO 42.22.01 are practically the same as those for 4C 39.25 (see Fig. 2).

Both sets of 10.7 GHz data can be fitted with single- and multi-component models extended in position angles near 0°. One-component models require major axes of length $\sim$0.″001 with very small axial ratios ($\lesssim$0.3). An angular size of 0.″001 corresponds to about 6 lt-yr at the distance of VRO 42.22.01. In view of the rapid 10.7 GHz flux density variations, with time scales less than two weeks (MacLeod *et al.* 1971), such an extended source seems unlikely; and we have investigated models with smaller components. Core-halo models require rather long ($\sim$0.″002) and thin

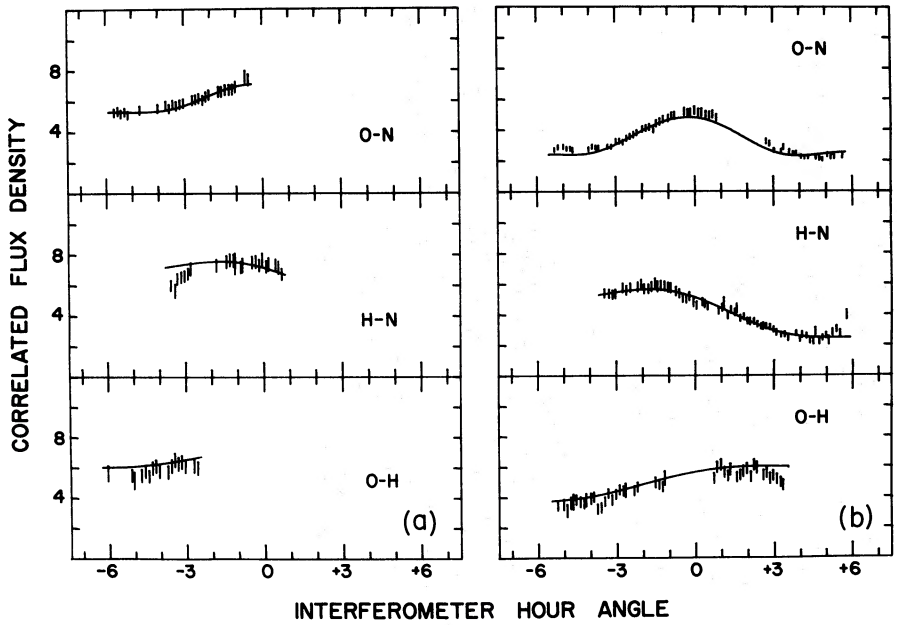

FIG. 5.—Fringe amplitude data for VRO 42.22.01. (a) = session 1, (b) = session 2. Scales and baselines as in Fig. 1. The solid lines are the calculated visibilities for the models described in the text.

($\lesssim 0''.0005$) halos, unlike any other model components in these Papers, except for the NRAO 150 elliptical Gaussian. Therefore, we have concentrated on double models.

Since the data from session 2 are much more extensive, we have used them to determine a model. It was then possible to fit a similar model to the session 1 data.

Session 2 is fitted reasonably well by an unequal double with separation $0''.0014$ in PA $\sim 0°$. The two components have sizes $\sim 0''.00045$ and an intensity ratio of 2.5. They account for the total 10.7 GHz flux density. A model with the same separation and position angle, but with an intensity ratio of 5.3 and a "point" for the stronger component, fits the data from session 1. Again, the model accounts for S_t. These models are represented by the solid lines in Figure 5. Observations of VRO 42.22.01 during session 3 were severely affected by weather, but they are consistent with these models. The position angle given here is probably accurate to a few degrees, but the component parameters (sizes, separations, and flux densities) are highly correlated and thus uncertain.

Our separation at 10.7 GHz is somewhat larger than that for the last two sessions of Clark *et al.* (1973), determined for an equal point double at 7.85 GHz ($0''.0010 \pm 0''.0002$ in April and June of 1972). However, an unequal double with greater separation would also fit the 7.85 GHz data, and the structure would be very similar at the two frequencies. The two components are perhaps identified with the sum of outbursts I, II, and III of Figure 3 of Andrew (1973). In that case, the flux density and size of the components evolved slowly between April and October of 1972, with little or no motion.

d) 3C 345

We have data for this source for only one baseline (OVRO–NRAO) and only from session 6. The data are given in Figure 6. The (u, v) track is the same as the OVRO–NRAO track for 4C 39.25 (Fig. 2).

It is possible to get a reasonable fit to the data with a point double model supplying about 7.3 Jy ($\sim 70\%$ of S_t). However, our more recent experiments (unpublished) at 10.7 GHz and 14.8 GHz, with much better (u, v) coverage, indicate that $\gtrsim 90$ percent of the total flux density comes from the two compact components. Accordingly, we have tried double models with more flux coming from partially resolved components. The fit we get is exceedingly good. The best-fitting model has a component separation of $0''.00123$ in PA 105°. The components are nearly equal in intensity and supply 9.6 Jy ($\sim 94\%$ of S_t). Their diameters are $\sim 0''.00055$. The separation and position angle are well determined, but the component sizes and intensity ratio are correlated and poorly determined without additional (u, v) coverage. The calculated visibility for this model is the solid line in Figure 6. The physical separation of the model components is ~ 30 lt-yr and the component sizes are ~ 12 lt-yr.

Cohen *et al.* (1971) found the same position angle for 3C 345 at 7.85 GHz in early 1971. Wittels *et al.* (1975) have extensive data for this source at 7.85 GHz for the two years preceding session 6. They also find the same position angle but a separation of $0''.00105$, with no indication of time variability. It appears that the component separation is different at the two frequencies, or the source structure changed in late 1973. Further observations at 3.8 cm are needed to settle the question.

e) 3C 454.3

We have extensive data for this source from session 2 only. The data are shown in Figure 7. The (u, v) tracks are given in Figure 8. We did not obtain the fullest possible coverage, but the minor variations in the visibility curves indicate that we probably did not miss much information. The source is only slightly resolved, and is best represented by a core-halo structure.

There is no unique core-halo model, however, since the sizes and fluxes of the model components are correlated. Typical models have cores $\sim 0''.0003$ (~ 7 lt-yr) contributing 7–8 Jy and halos $\sim 0''.0015$ which supply ~ 2 Jy. The solid line in Figure 7 represents a core-halo model. Observations at higher resolution are necessary to determine if the source is more complex.

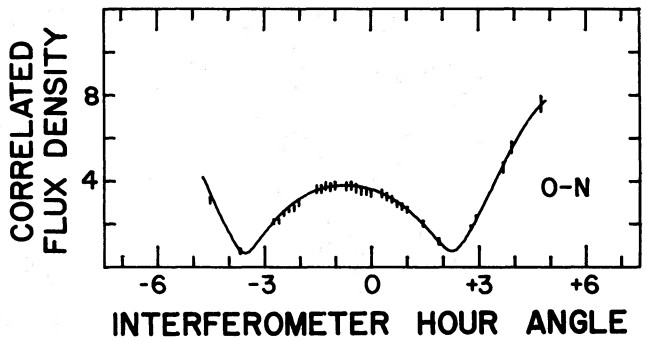

FIG. 6.—Fringe amplitude data for 3C 345 for the OVRO-NRAO baseline in session 6. Scales as in Fig. 1. The solid line is the calculated visibility for the model described in the text.

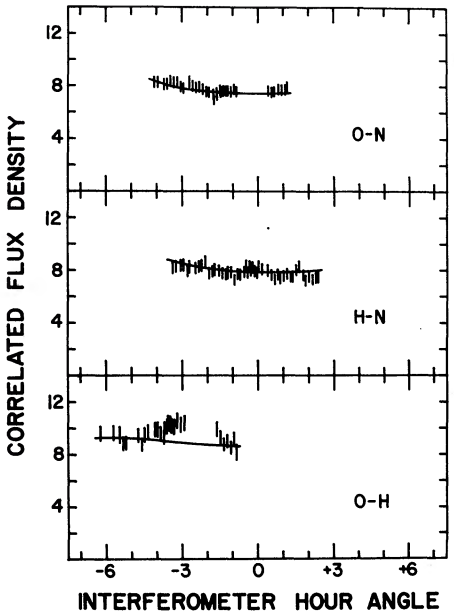

FIG. 7.—Fringe amplitude data for 3C 454.3 for session 2. Scales and baselines as in Fig. 1. The solid lines are the calculated visibilities for a typical core-halo model, as described in the text.

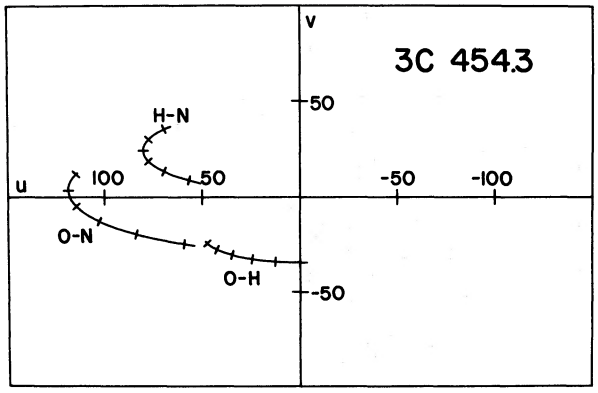

FIG. 8.—(u, v) tracks for 3C 454.3. Scales as in Fig. 2.

We have higher resolution data from session 5 between OVRO and MPI, but the intermediate baselines HRAS–NRAO and OVRO–NRAO are missing. Between sessions 2 and 5, the total flux density dropped from 12.1 to 9.0 Jy. The correlated flux density also fell by about 3 Jy to 6–7 Jy on the short OVRO–HRAS baseline. We observed ~ 2 Jy on the OVRO–MPI baseline at $290 \times 10^6\lambda$ during session 5. It seems reasonable to ascribe the decrease in total flux density to the core component. In that case, the ~ 2 Jy observed between OVRO and MPI indicates a size of $\sim 0''.0003$ for the core, or about the same as the session 2 models, and is consistent with a simple structure for the source.

Radio outbursts of 3C 454.3 in 1965 (Kellermann and Pauliny-Toth 1968) and 1971 (Dent and Kojoian 1972; Dent and Hobbs 1973) make it difficult to compare these results with earlier VLB measurements. Those observations, from 607 MHz to 7.85 GHz (Purcell 1973; Kellermann *et al.* 1971; Cohen *et al.* 1971), suggest a series of several (concentric?) core-halo components ranging in size from $\sim 0''.01$ to $\lesssim 0''.0004$. Wittels *et al.* (1975) have used double models to match their observations at 7.85 GHz, but at 10.7 GHz our data do not show any evidence for either of their models.

III. CONCLUSIONS

Most, if not all, of the sources consist of multiple components. However, the sources seem to be fairly simple, and only two components are needed to reproduce the major features of the visibility curves. Simple models, chosen because they require the fewest parameters, suffice to fit the data very well. More extensive data may reveal greater complexity. The models are similar in appearance to the maps of more extended (by a factor of 10^4–10^5) sources.

For the double sources with redshifts (4C 39.25, 3C 345, VRO 42.22.01), the component separations range between about 10 and 50 lt-yr. Typical component sizes are on the order of 10 lt-yr, within a factor of 2. The smallest components appear to be in VRO 42.22.01, with diameters $\lesssim 2$ lt-yr. This source is also the most rapid variable under discussion here. The components of most of the sources considered in Paper III, which have more rapid variations, are also smaller than most of the components discussed in this paper.

Most of the sources discussed here have similar structure at 10.7 GHz and 7.85 GHz. Typically, the orientation of the source is the same at the two frequencies, but the component separations and intensity ratios are different. The sources presumably consist of discrete components with frequency-dependent shape and strength. These experiments and others at nearby frequencies should allow us to determine the nature of individual compact components and to follow their evolution.

It is unknown if the individual components have a common or separate origin. Our experiments would be sensitive to component separations up to $0''.02$. We do not see such widely separated components at 10.7 GHz in any of our sources, indicating that the production of high-frequency compact components is well localized to regions $\lesssim 50$ lt-yr across. The larger scale sources seen at lower frequencies ($\sim 0''.01$ at 408 MHz and 607 MHz: Clarke *et al.* 1969; Purcell 1973) are either intermediate stages of radio source evolution or different kinds of outbursts.

The sources discussed in these papers have nearly all their 10.7 GHz radiation coming from compact components. These sources are also among the strongest extragalactic objects at this frequency. The other strong sources are extended radio galaxies (which may also have weak compact cores). This dichotomy must be explained by any theory of radio source evolution.

We must caution against statistical overinterpretation of our results. The sources are few in number and were chosen for the likelihood of interesting results. They are not a complete sample of any kind.

The acknowledgements of Paper I are reaffirmed here, especially to the ARO observers for preliminary flux densities for most of our sessions. We also thank G. Purcell for his extensive help with session 6.

REFERENCES

Andrew, B. H. 1973, *Ap. J.* (*Letters*), **186**, L3.
Baldwin, J. A., Burbidge, E. M., Robinson, L. B., and Wampler, E. J. 1975, *Ap. J.* (*Letters*), **195**, L55.
Clark, B. G., Kellermann, K. I., Cohen, M. H., Shaffer, D. B., Broderick, J. J., Jauncey, D. L., Matveyenko, L. I., and Moiseev, I. G. 1973, *Ap. J.* (*Letters*), **182**, L57.
Clarke, R. W., Broten, N. W., Legg, T. H., Locke, J. L., and Yen, J. L. 1969, *M.N.R.A.S.*, **146**, 381.
Cohen, M. H., Cannon, W., Purcell, G. H., Shaffer, D. B., Broderick, J. J., Kellermann, K. I., and Jauncey, D. L. 1971, *Ap. J.*, **170**, 207.
Cohen, M. H., Moffet, A. T., Romney, J. D., Schilizzi, R. T., Shaffer, D. B., Kellermann, K. I., Purcell, G. H., Grove, G., Swenson, G. W., Yen, J. L., Pauliny-Toth, I. I. K., Preuss, E., Witzel, A., and Graham, D. 1975, *Ap. J.*, **201**, 249 (Paper I).
Dent, W. A., and Hobbs, R. W. 1973, *A.J.*, **78**, 163.
Dent, W. A., and Kojoian, G. 1972, *A.J.*, **77**, 819.
Kellermann, K. I., Jauncey, D. L., Cohen, M. H., Shaffer, D. B., Clark, B. G., Broderick, J., Rönnäng, B., Rydbeck, O. E. H., Matveyenko, L., Moiseyev, I., Vitkevitch, V. V., Cooper, B. F. C., and Batchelor, R. 1971, *Ap. J.*, **169**, 1.
Kellermann, K. I., and Pauliny-Toth, I. I. K. 1968, *Ann. Rev. Astr. and Ap.*, **6**, 417.
MacLeod, J. M., Andrew, B. H., Medd, W. J., and Olsen, E. T. 1971, *Ap. Letters*, **9**, 19.
Oke, J. B., and Gunn, J. E. 1974, *Ap. J.* (*Letters*), **189**, L5.
Purcell, G. H. 1973, Ph.D. thesis, California Institute of Technology.
Schilizzi, R. T., Cohen, M. H., Romney, J. D., Shaffer, D. B., Kellermann, K. I., Swenson, G. W., Yen, J. L., and Rinehart, R. 1975, *Ap. J.*, **201**, 263 (Paper III).
Shaffer, D. B., Cohen, M. H., Jauncey, D. L., and Kellermann, K. I. 1972, *Ap. J.* (*Letters*), **173**, L147.
Wittels, J. J., Knight, C. A., Shapiro, I. I., Hinteregger, H. F., Rogers, A. E. E., Whitney, A. R., Clark, T. A., Hutton, L. K., Marandino, G. E., Niell, A. E., Rönnäng, B. G., Rydbeck, O. E. H., Klemperer, W. K., and Warnock, W. W. 1975, *Ap. J.*, **196**, 13.

M. H. COHEN, J. D. ROMNEY, and R. T. SCHILIZZI: Astronomy Department, California Institute of Technology, Pasadena, CA 91125

K. I. KELLERMANN and D. B. SHAFFER: National Radio Astronomy Observatory, Green Bank, WV 24944

R. RINEHART: Harvard Radio Astronomy Station, Fort Davis, TX 79734

G. W. SWENSON, JR.: University of Illinois Observatory, Urbana, IL 61801

J. L. YEN: University of Toronto, Toronto 5, Ontario, M5S 1A7, Canada